High performance MRI simulation of arbitrarily complex flow: A versatile framework

Alexandre Fortin, Stéphanie Salmon, Joseph Baruthio, Maya Delbany, Emmanuel Durand

High performance MRI simulation of arbitrarily complex flow: A versatile framework

Fortin A.[a], Salmon S.[a], Baruthio J.[b], Delbany M.[b], Durand E.[c]

[a]*Laboratory of Mathematics, URCA, Reims, France*
[b]*ICube, University of Strasbourg, UMR 7357, CNRS, FMTS, France*
[c]*IR4M, University Paris-Sud XI, UMR 8081, CNRS, France*

Abstract

PURPOSE: During the last decades, magnetic resonance angiography has been used as a clinical routine for precise and non-invasive exploration of vessels, as well as for diagnosis of the most current neurovascular diseases. Several dedicated codes were developped to simulate specifically the process of arbitrarily complex flow imaging. Though, currently, most of the most advanced and performing MRI simulators do not include this option and are specialized in static tissues imaging. This work was carried out to expand the possibilities of one of those software in order to propose a complete full-featured tool for simulation of any MR experience including fluid motion.

THEORY AND METHODS: We present here an extension of JEMRIS, which is currently a performing and prevalent open-source software for MRI simulation. By implementing a Lagrangian description of individual spins motion, we are able to simulate any MR experience including both static tissues and arbitrarily complex flow.

RESULTS: We show the efficiency of this approach by replicating some specific angiographic pulse sequences such as phase contrast velocimetry, Time-of-Flight sequence or contrat agent injection. We also reproduce the appearance of flow artifacts (misregistration) on usual sequences. Those results include flow data based on theoretical flow model as well as complex numerical data obtained from Computational Fluid Dynamics methods.

CONCLUSION: We get an efficient and versatile tool for simulation of any MRI experience including physiological fluids with arbitrarily complex flow motion.

Keywords: MRI simulation, Bloch equations, angiography, complex flow, CFD, JEMRIS

1. Introduction

Since its beginnings [1], MRI simulation has proven to be an effective tool for numerous research fields. We can cite, e.g., design of pulse sequences, testing of physical models, development of new methods or even educational purposes [2].

For simulation of realistic experiences, the effect of physiological circulating fluids, such as blood flow or lymph, is of crucial importance as it has been shown that those motions can induce numerous artifacts and lead to a deterioration of the image quality and to interpretation errors. Moreover, including flow motion into an MRI simulator is obviously a necessary condition to study specific angiographic methods such as contrast agent injection, phase-contrast velocimetry or time-of-flight pulse sequences. This could also be an efficient tool for exploration of perfusion and spin labeling techniques.

Several techniques were developed to simulate specifically the whole physical process of MR angiography, coupled with Computational Fluid Dynamics (CFD) methods. Those techniques can be classified as Lagrangian [3], Eulerian [4] and mixed approaches [5], depending on the way to express and solve Bloch equations.

However, the most advanced and versatile MRI simulators to date are widely specialized in static tissues simulation and most of them do not include any option for blood flow modeling. This is the case, e.g., for SIMRI [6], ODIN [7] and POSSUM [8]. ODIN is specialized in simulation of diffusion phenomena, based on Bloch-Torrey equations. POSSUM can simulate fMRI and rigid motion of the object. More recently, MRISIMUL shows the ability to simulate laminary flow motion from analytical velocity expression [9].

The main limitation of such simulators is that they are not intended natively to deal with complex flow data from CFD. The other point is that they are widely based on analytical time-discretized solutions of Bloch equations, which imposes some limitations on the MRI pulse-sequence and prohibits the use of complex nonlinear RF waveforms and gradients.

JEMRIS is, from this point of view, one of the most full-featured simulation platform, including easy and complete pulse sequence design tools with arbitrary waveforms [10]. As most MRI simulators, it is based on isochromat summation method[1], with a numerical approach. Bloch equations are

[1]In this context, the terms "isochromat", "spin" and "particle" are used as

solved with an independent solver library for Ordinary Differential Equation (ODE) systems, based on Adams-Moulton linear multistep method. Thus, no limitation is imposed on the pulse sequence waveforms. An exhaustive list of physical effects involved in the imaging process are also taken into account, as e.g. non-uniform gradients, chemical shift, field inhomogeneities (T2*), concomitant gradient fields, Gaussian white noise or magnetic susceptibility effects. Natively, JEMRIS can also simulate rigid motion of the sample, but no individual particles trajectories.

We aimed to extend the possibilities of this prevalent software in order to simulate arbitrarily complex flow motion data obtained from analytical velocity expression or from CFD. We thus propose a versatile framework for realistic simulation of any complex MR experience inluding both static tissues and physiological circulating fluids, e.g. angiographic sequences or flow artifacts study. The advantages inherited from JEMRIS allow to reproduce any pulse-sequence type, even those including nonlinear RF waveforms or time-varying gradients, contrary to simulators based on analytical methods.

We first give a brief overview of the theoretical bases of MRI flow simulation. Thus, we justify the implementation of a Lagrangian method in JEMRIS as the simplest way to simulate angiographic experiences. Then, we describe the conditions to impose on the trajectories and choice of parameters for physically realistic simulations. Finally, we show the efficiency of our framework by presenting a set of results simulated with the three main classical angiographic techniques (Phase Contrast, Time-Of-Flight and contrast agent injection) and a well-known flow artifact (misregistration) and we establish comparisons with some experimental acquisitions on a physical phantom. The results include both static tissues and flow simulations, with trajectories generated synthetically from analytical velocity expression or from CFD data with particle tracking methods.

2. Theory

Several approaches have been proposed to simulate angiographic images, and more generally all MR experiences including flowing particles. We can classify them into Lagrangian, Eulerian and mixed methods.

2.1. Lagrangian approach

Lagrangian methods use the same approach to describe flowing particles as that typically used for simulation of static tissue images [3]. Classical expression of Bloch equations, based on total particle derivative, is solved individually for each isochromat to get the value of the macroscopic magnetization $\mathbf{M}(t)$ of the particle along its trajectory:

$$\frac{d\mathbf{M}}{dt} = \gamma \mathbf{M} \times \mathbf{B} - \hat{\mathbf{R}}(\mathbf{M} - \mathbf{M_0}) \tag{1}$$

where $\mathbf{M}$ is the magnetization vector of the isochromat, $\mathbf{M_0}$ is the steady state value of magnetization, γ is the gyromagnetic ratio of hydrogen, $\mathbf{B}$ is the external magnetic field and $\hat{\mathbf{R}}$ the relaxation matrix with T_1 and T_2 relaxation times.

$$\hat{\mathbf{R}} = \begin{pmatrix} 1/T_2 & 0 & 0 \\ 0 & 1/T_2 & 0 \\ 0 & 0 & 1/T_1 \end{pmatrix}$$

Lagrangian method is the most intuitive technique to simulate flow motion, as it closely mimics the physical process of fluid circulation. Its main advantage is the ease of resolution of Bloch equations, which are a simple ODE, and the possibility to implement analytical time discretized solutions in the algorithm (with some restrictions on the pulse-shape sequence). Moreover, flowing particles need not a specific processing, compared to static tissues. Another asset is the possibility to easily simulate specific experiences with heterogeneous fluid interactions, such as contrast agent injection in the blood system. The main constraint is the necessity to determine the flowing particles trajectories with an acceptable degree of accuracy, as lack or accumulations of spins in some regions lead to signal blanks or peaks in the final image.

2.2. Eulerian approach

Eulerian methods are based on formalisms inspired from fluid mechanic. Magnetization is hence considered as a field depending on space and time $\mathbf{M}(\mathbf{r}, t)$. Bloch equations are expressed from an Eulerian point of view by replacing in Eq. 1) the expression of the total particle derivative by the corresponding Eulerian partial derivatives:

$$\frac{d\mathbf{M}}{dt} = \frac{\partial \mathbf{M}}{\partial t} + (\mathbf{V}.\nabla)\mathbf{M} \tag{2}$$

where $\mathbf{M}$ is the magnetization vector of the tissue and $\mathbf{V}$ is the velocity of the flowing spins at the considered point. The Partial Derivative Equation (PDE) can then be solved on a mesh to get the value of magnetization over time on a discrete collection of points in the sample [11] [4]. The main advantage of this technique is that both Bloch and Navier-Stokes equations can be solved successively on the same mesh. Therefore, there is no need to compute individual particles trajectories, which can be a computationally expensive step. The main disadvantage is the complexity of PDE solving, which requires specific knowledge, and the heaviness of the method for simulation of samples including both static tissues and flowing particles.

2.3. Mixed approach

We could classify as "mixed" methods all those proposing an intermediate solution beetwen both previous methods. For instance, some iterative approaches propose to calculate the value of magnetization in a collection of fixed points by separating Bloch evolution of the spin from fluid advection phenomena [5]. Bloch equations are iterated at each fixed point as first step, and the value is then translated to neighboring points, proportionally to the local velocity. The main advantage of those physically intuitive methods is that they avoid the need

synonymous.

to calculate particles trajectories separately. As for Lagrangian methods, the equations to solve are a simple ODE system, however an additional step is needed in the simulation to consider the advection of magnetization due to the fluid motion.

3. Methods

We chosed a Lagrangian approach for our framework. Its flexibility allows an easy implementation in an advanced simulator based on isochromat summation method, such as JEMRIS. This it is the simplest way to get a versatile tool, able to simulate complex samples without specific technical knowledge.

3.1. Flow simulation

Natively, JEMRIS is only dedicated to static tissues, with optional rigid motion of the sample.

MR signal is obtained by solving Bloch equation for each isochromat individually. No analytical time-discretized solution is implemented. Differential equations are solved independently with the numerical library CVODE froms Sundials. ODE solving is based on Adams-Moulton linear multistep method. The desired level of precision for ODE resolution can be modified in the code. The choice of an independent solver authorizes to use any pulse-shape sequence with arbitrary complex waveforms, whereas simulations based on analytical solutions are generally limited to piecewise constant gradient fields and RF pulses.

The use of the Lagrangian approach to simulate flow motion requires to determine the trajectory of each individual spin. While solving Bloch equations, this method avoids the need to use a different treatment for static tissues and flowing particles. We simply vary the position of the spin over time, which modifies the field value seen by the particle:

$$\mathbf{r} = \mathbf{r}(t) \Rightarrow \quad \mathbf{B}(\mathbf{r}, t) = [\mathbf{G}(t).\mathbf{r}(t) + \Delta B(\mathbf{r}, t)].\mathbf{e_z} + \mathbf{B_1}(\mathbf{r}, t)$$

where $\mathbf{G}(t)$ is the gradient sequence, $\mathbf{r}$ is the isochromat position, $\Delta B(\mathbf{r}, t)$ is the field inhomogeneity due to off-resonance and non-uniform gradients, and $\mathbf{B_1}(\mathbf{r}, t)$ the RF pulse sequence.

By default, JEMRIS only allows to submit one trajectory for the whole sample, in order to simulate rigid motion. We provide an extension to the software in order to simulate fluid travelling. A specific class was added to the C++ code to allow users to specify each individual spin trajectory.

With this new version, it thus becomes possible to describe flow phenomena, after converting data to the proper format, i.e. date/position of each spin successively over the whole sequence duration.

3.2. Dynamic isochromats settings

The description of the flow in terms of Lagrangian trajectories supposes some conditions for realistic simulations.

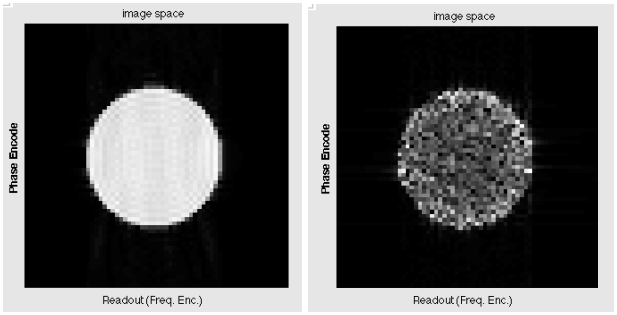

Figure 1: Effect of an irregular spatial distribution of spins $\rho_{isochromats}(\mathbf{r})$. Here is a GRE simulation of laminar flow (cross-section), with resolution 128 and mean density of $2, 6$ spins per voxel in the readout and phase directions. Left: Isochromats regularly distributed over space. Right: Isochromats randomly distributed over phase and readout direction (but regularly distributed along flow axis). As we can see, the non constant spatial distribution of particles is responsible for signal peaks and gaps on the magnitude image.

Trajectories format. Individual trajectories of the spins are stored in a separate file. Each trajectory is described successively, by specifying a discrete collection of positions of the particle at different significant time points over the pulse sequence. Intermediate positions are then determined by linear interpolation. However, there is no restriction on the timestep interval, which can be chosen as short as desired, for a precise description of any arbitrarily complex flow trajectory. Obviously, the number of significant positions can be reduced to describe the straight parts of the trajectories. The timestep need not be constant over time and particles, and is hence entirely at the appreciation of the user.

Continuous flow. For simulation of physically realistic phenomena, such as blood circulation, a continuous flow of particles is required during the whole duration of the pulse sequence. Of course, the vessel geometry must already be filled at the beginning of the sequence. However, for simulation of periodic flow motion, e.g. due to heartbeat, the same trajectories can be reused periodically.

Isochromats density. To accurately simulate the final MR signal with discretely distributed points, a sufficient number of isochromats per voxel is necessary. At least one isochromat per voxel is needed to get a consistent image of the sample. However, it has been shown that at least two isochromats per voxel and direction are needed to get an error lower than 3,5% on the calculated signal, and that three isochromats per voxel and direction are needed to get an error lower than 1,5% [12].

Classically, for simulations based on isochromat summation method, the spatial interval between neighboring isochromats is supposed to be constant in the sample. The same way, for simulation of incompressible fluids, the quality of flow models used must ensure that the spins density will incur few variations over space and time. This means that trajectories calculated must prevent lack of spins or accumulations in a voxel:

$$\rho_{isochromats}(\mathbf{r}, t) \approx cte$$

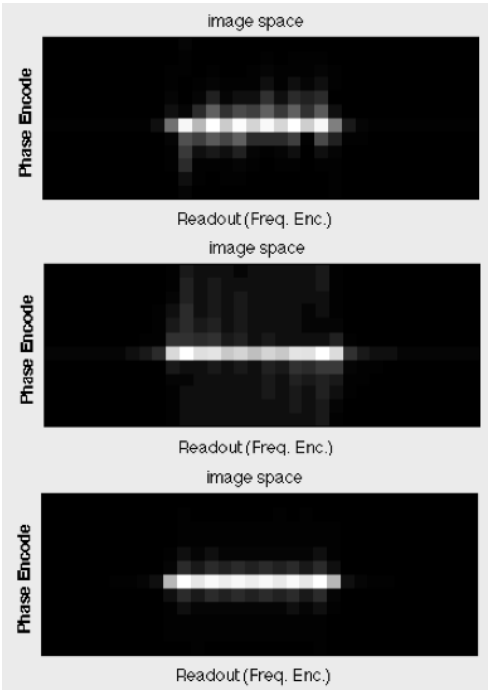

Figure 2: Spurious echoes on spoiled sequence for various isochromats density. GRE sequence including spoiling gradients, with TR = 40 ms, TE = 20 ms, $T2$ = 50 ms and RF angle set to 20°. Above: 3 isochromats per voxel in the readout direction. Middle: 10 isochromats per voxel in the readout direction. Below: 50 isochromats per voxel in the readout direction. The bad quality of the above image with $T_2 > TR$ indicates that remaining transversal magnetization in a voxel is not properly destroyed by the spoiling gradients for low isochromats density, with possible accidental refocusing.

where $\rho_{isochromats}(\mathbf{r}, t)$ is the density of static and dynamic isochromats at a given time and position.

A too much irregular distribution of spins could, indeed, lead to artificial signal peaks or lacks in some regions (Fig. 1).

However, in the case of data obtained from CFD, e.g. to study flow through complex vessel geometries, it can be difficult in practice to get a set of Lagrangian trajectories preserving a constant spatial distribution of spins throughout the experience. Indeed, previous studies on particle tracking suggest that even with higly resolved CFD mesh and high Lagrangian particles density, a uniform distribution of spins at inlet never remains perfectly uniform flowing throughout a complex geometry [13]. Increasing the density of particles can circumvent the problem but will result in higher execution times. In that case, some specific solutions have to be developed to preserve a uniform density, as the software do not intend to control the characteristics of flow data used as input or to correct potential density inhomogeneities.

Spoiling gradients. Another restriction will appear with some specific pulse sequences, resulting from the use of particles with discrete spatial localization. Indeed, simulation of spoiling gradients can lead to the appearance of some artificial spin echoes and, finally, to numerical artifacts on the image (Fig. 2). Contrary to biological tissues with continuous distribution of spins, spoilers will not necessary destroy transversal residual magnetization, as a discrete spatial repartition of isochromats can lead to constructive magnetization vectors summation inside a voxel [14]. Some simulators workaround by calculating specific intravoxel spins dephasing [7] or by nulling transversal magnetization automatically when a spoiling gradient is applied [15]. Again, an increased density of particles can circumvent the problem but will extend execution times.

Total number of isochromats. Finally, for each experience with incompressible flow, the total number of required dynamic spins $N_{dynamic}$ is given by :

$$N_{dynamic} = (V_{geometry} + Q \times T_{sequence}) \; / \; (\delta x.\delta y.\delta z)$$

where $V_{geometry}$ indicates the total inner volume of the vessels geometry, Q denotes the total inflow rate, $T_{sequence}$ is the total duration of the experience and $\delta x, \delta y, \delta z$ denote the mean spatial interval between neighboring isochromats. As the number of isochromats can rapidly increase for experiences with high values of blood flow rate, the resolution of the sequence and the spatial density of isochromats in a voxel shall be chosen carefully.

Spins storage. Before the spins enter the Region Of Interest (ROI), and after they leave it, dynamic spins can often be stored in a static place. In most cases, e.g. when the motion is oriented normally to the slice, the particles can not be immobilized just after they left the slice, because motion after slice excitation can be responsible for important physical effects on the final image (flow artifacts, specific spins dephasing). In fact, motion must be simulated at least until next readout, to take into account all the specific effects of gradients on moving spins. For most pulse sequences, it is not useful to simulate particles motion after TE, because residual signal will be neglectable on the next acquisition line if the remaining transversal signal has been treated properly. The thing to notice is that any flowing spin excited with an RF pulse can still produce physically significant signal, even once it left the slice.

Besides, the flowing particles must not disturb the rest of the image with spurious signal when they are stored in a static place outside of the ROI. Three solutions provide good results:

- The first possibility is to collect only the signal present in the ROI by selecting a specific spatial volume with the antenna. Thus, any spurious signal from flowing particles outside of the ROI is filtered numerically. Thereupon, Jemris proposes natively a tool for antenna design and location, with adjustable spatial sensibility extent.

- The second solution is to store the dynamic spins in a place so that they will not incur the RF excitations before they begin their movement after they complete it.

- The last possibility is to null artificially the signal of the dynamic isochromats when they are outside of the ROI.

In summary, for realistic simulations, the following points should be considered carefully:

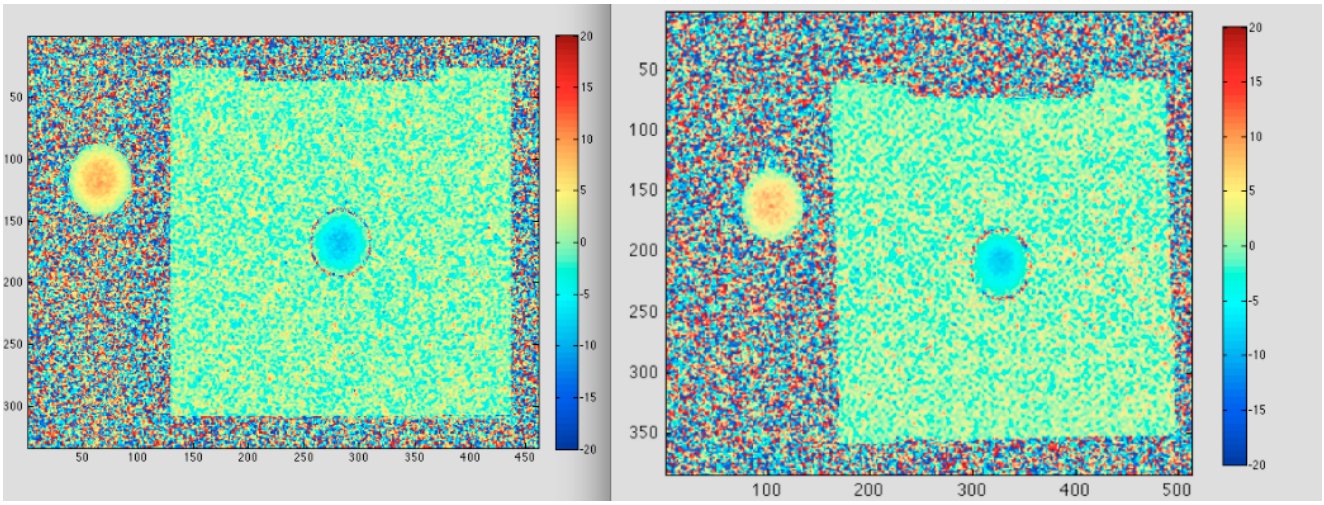

Figure 3: Phase contrast velocimetry. Comparison between JEMRIS simulations and experimental images of a physical flow phantom. At the center of both images, flexible tube with steady laminary flow, immersed in static water. On the left of the images, return line with steady laminary flow.

1. Lagrangian description of all successive positions of the flow particles over the sequence, with arbitrary time step.
2. Vessel geometry filled at t=0 and all over the sequence with a continous flow of particles.
3. Constant density of particles over time and vessel position $\rho_{particles}(\mathbf{r}, t) \approx cte$, i.e. no lack or accumulations of spins.
4. At least one spin per voxel and direction, ideally three.
5. Storage of the flowing spins in a place where they do not produce any spurious echo. Prolongation of the motion outside of the slice until next readout.
6. For sequences including spoiling gradients, sufficient spins density to avoid accidental spins rephasing in a voxel.

3.3. Hardware implementation

JEMRIS proposes a parallel mode via MPI. The sample to be imaged is divided into subsamples, distributed among CPUs. Computation time greatly depends on the content of the pulse sequence and on CVODE module performances. Hence, there is not a simple linear relation between computation time and pulse sequence duration, contrary to simulators based on time-discretized solutions. Otherwise, we observe a proportional relation between CPU numbers and computation time.

Our simulations are performed with parallel supercomputer[2], and about a hundred of CPUs for each experience.

All the positions of the spins trajectories $\mathbf{r}(t)$ are coded on 4B with float variables, which leads to a range of value between $-3,4.10^{-38}$mm and $3,4.10^{38}$mm. Therefore, the significant digits are coded on 23 bits, the exponent on 8 bits and sign on 1 bit, which lead to a precision of 6 digits to the right of the decimal point. By default, positions are expressed in millimeters. For typical angiographic experiences, with particles motions of a few centimeters, this means almost a nanometric precision ($\sim 10^{-8}$m) for the description of the particles trajectories. However, the type of variable can easily be replaced in the C++ code with double precision or long double for specific experiences demanding a higher precision level.

[2]ROMEO HPC center, hosted by the University of Reims Champagne-Ardenne.

4. Results

We present here some current angiographic experiences carried out to show the ability of JEMRIS to simulate flow phenomena efficiently, in parallel with static tissues. Two experiences are carried out on a straight tube and compared with experiments made on a physical phantom. Here, the trajectories are synthetized from simple analytical velocity expressions of the flow.

4.1. Experimental flow phantom

Our experimental flow phantom is an hydrodynamic bench with a flexible tube inside the bench and a rigid tube as return line. The flexible tube has an inner diameter of 19 mm at rest and a thickness of 1,04 mm. The pipe wall reproduces compliance of an artery [16] (0,32%/mmHg) and is immersed in static water to avoid deformations effects from gravity. For phase contrast experiences, Glycerol is injected in the flowing water to get a dynamic viscosity of $2,4.10^{-3}$ Pa.s. Therefore, we are close to blood viscosity at 37°C and we can reach more easily the laminary flow conditions. All experiences presented here are carried out with steady flow, but unsteady flow patterns can also be simulated with the same method.

Images were acquired on a 3T Siemens machine.

4.2. Phase contrast velocimetry

The implementation of a Lagrangian description of flow in JEMRIS allows us to easily simulate complex experiences including both static structures and flow. Though, we are able to

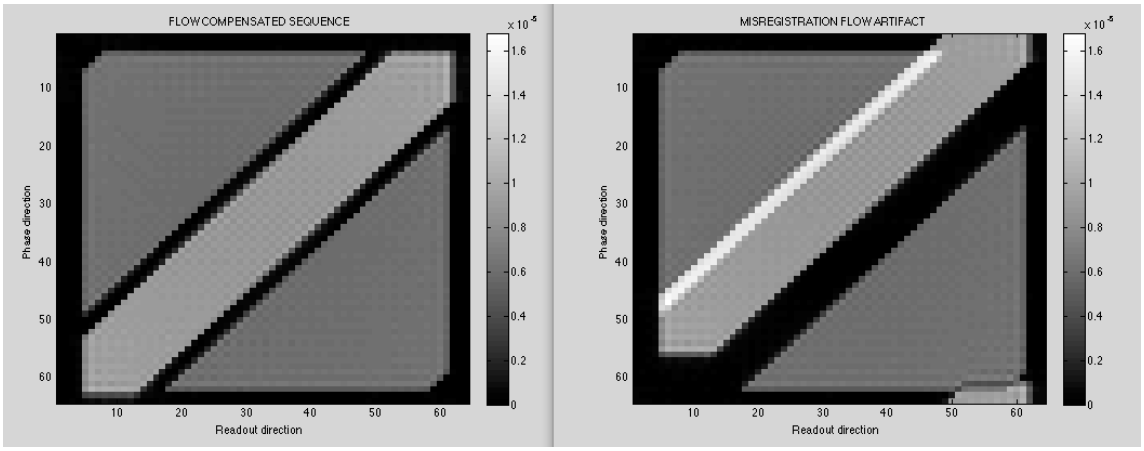

Figure 4: Flow artifacts. JEMRIS simulations of a standard displacement artifact. (Left) corrected and (Right) uncorrected pulse sequence.

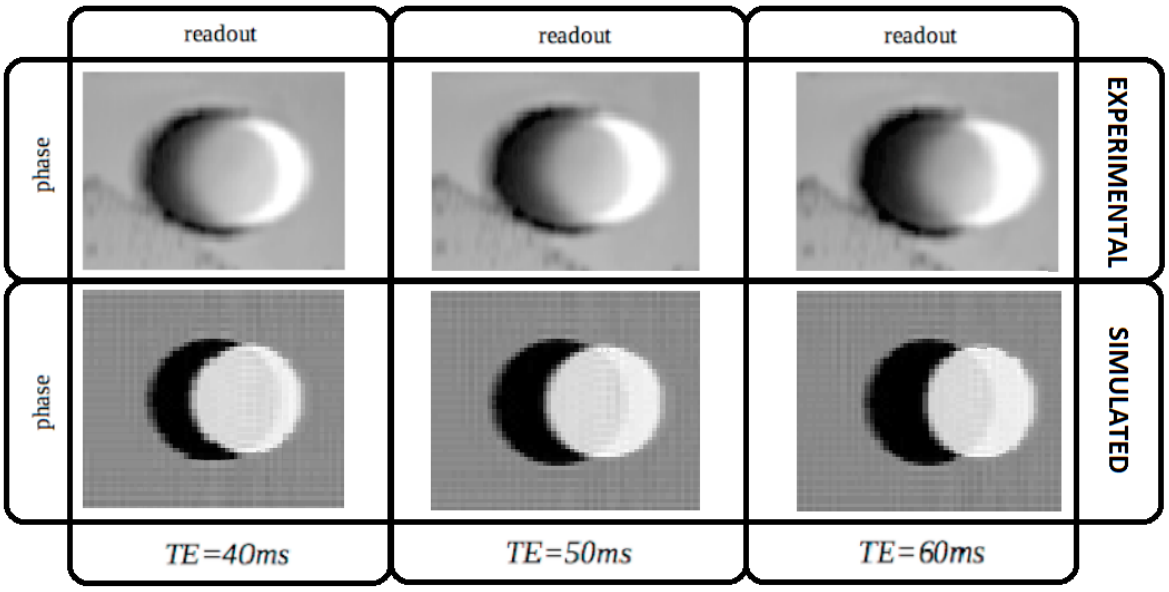

Figure 5: Flow artifacts. Comparison between JEMRIS simulations and experimental images for a non-standard displacement artifact in the readout direction, with oblique flow through the slice, for various TE delays.

reproduce phase contrast acquisitions on the experimental flow phantom.

Phase contrast is a well-known non-invasive angiographic technique for velocimetric measurements [17]. We perform here 1D-velocity encoding with flow going through the slice, in the z-direction. Velocity is encoded by adding a bipolar gradient in the slice direction on a classical GRE pulse sequence. Sequence is run twice, with opposite bipolar gradient sign, leading to a dephasing:

$$\Delta\Phi = \gamma V_0 G \tau^2$$

where $\Delta\Phi$ is the motion-induced spin dephasing, γ is the gyromagnetic ratio of hydrogen, V_0 is the velocity of the spin at the considered point, approximated to be constant during the application of the bipolar gradient, G is the amplitude of the first lobe of the bipolar gradient and τ is the half-duration of the bipolar gradient.

We consider a simple laminar flow in a straight tube, thus spins velocity follows the Poiseuille law. We took Vmax = 88 mm/s at the center of the tube. Our 2D matrix was 461 × 333, resolution was set to 256, slice thickness was 2.5 mm and maximum velocity encoding Venc = 200 mm/s. TE was 10 ms, TR was 16 ms and RF pulse angle was 15°. The total number of spins was 2 069 943 and the inter-spins distance was 0,3 mm in the slice and 1,5 mm normally to the slice. Calculation took about 5,5 hours with 150 CPUs. A Gaussian white noise was then added randomly to the calculated signal. Phase images are obtained by complex division [18].

The experimental hydraulic flow rate was 114,8 mL/s. The experimental 2D matrix was 512 × 384, resolution was set to

256, slice thickness was 0,1 mm, TR was 55,1 ms, TE was 8,3 ms, RF pulse angle was 15° and NEX was 1.

We found a good agreement for the velocity values between experimental and simulated data (Fig. 3).

4.3. Misregistration Artifact

The standard misregistration artifact, or displacment artifact is a well-known motion-induced artifact, generally corrected on modern machines. On images of in-plane oblique vessels, it results in an error of location of the flowing spins on the image (Fig. 4) due to the motion of particles between phase encoding gradient and readout gradient [19].

We present here the simulation of a specific misregistration artifact, which appear when a vessel is going through a 2D-slice with an oblique angle. Thus, blood excited during the slice selection will continue its motion and its final position will be encoded during phase and readout gradients. Consequently, misregistration can appear in the readout and phase direction, depending on the orientation of the tube. It is important to notice that this artifact can persist even with classical flow compensation mechanisms. Here, displacement in the readout direction is directly proportional to the TE delay, which is generally not the case for classical misregistration artifact. For a straight tube with steady flow, inclined by the angle α to the slice in the readout direction, the apparent displacement Δx of a particle with constant velocity V_0 is given by :

$$\Delta x = V_0.TE.sin(\alpha)$$

Fig. 5 presents a comparison between simulations and experimental images of this non-standard displacement artifact in the readout direction, for three different TE delays.

For this simulation, we used a simplified model of perfect fluid with uniform velocity $V_0 = 366$ mm/s. The tube had an inner diameter of 20 mm and was inclined by $30,2°$ in the readout direction. The distance between neighboring isochromats was 0,6 mm and we used a total of 2 611 698 particles. The sequence used was a classical GRE. The 2D acquisition matrix was 64×64, resolution was 128, slice thickness was 5 mm, TR was 66 ms and NEX was 1. Simulation took only 68 minutes in parallel.

The experimental hydraulic flow rate was 114,8 mL/s in a tube of 20 mm in diameter, inclined by $30,2°$ in the readout direction. Experimental FOV was $246 \times 184,5$ mm, 2D acquisition matrix was 576×432 (i.e., real resolution was 234), slice thickness was 5 mm, TR was 66 ms, RF pulse angle was 15°, NEX was 32 and flow compensation mode was active.

We found a good agreement with the theoretical value of displacement, both for experimental images and simulated ones (see Fig. 5 and Tab. 1).

TE (ms)	Theoretical (mm)	Simulated (mm)
40	11	10,9
50	9,2	9,4
60	7,4	7

Table 1: Apparent displacement for different TE values.

5. Discussion and conclusion

We presented an open-source and extensible work for high performance MRI simulation of any experiment including fluid particles. This covers, inter alia, the field of angiographic acquisition as well as the study of flow effects on classical pulse sequences.

The main advantages of the Lagrangian approach chosen to describe the flow are the simplicity of implementation that does not require specific knowledge and the possibility to carry out realistic simulations of large samples including both static tissues and arbitrarily complex flow motion. As it closely mimics the physical process of fluid circulation, the injection of some specific substances such as contrast agent can be directly reproduced.

Simulations can take as entry synthetic flow data from theoretical flow models as well as numerical flow data from CFD, for simulation of blood flow in realistic complex vessels geometry. Other simulators have already proposed some results for flow simulation, but they generally only concerned data from analytical velocity expression [9] or they only deal with a very specific type of acquisition. Some of them are exclusively centered on flow simulation study [3, 4, 5] or only reproduce a specific type of pulse sequence [20]. Contrarily to specialized codes, choosing to extend a pre-existing high performance MRI simulator allows to get few limitations on pulse sequence type, neither than on fluid and tissues nature. Moreover, no restriction is imposed on flow timestep precision as JEMRIS kernel is based on a numerical solving of Bloch equations contrarily to other simulators commonly based on a time-discretized analytical solution. Parallelization allows to perform simulations of large samples with reduced time consumption. All those characteristics lead to a tool offering a very high degree of versatility.

Combining this work with all the existing possibilities of the original software, JEMRIS is today one of the most performing and versatile tool for simulation of any complex MRI experience.

6. Acknowledgements

We sincerely thank JEMRIS developers to provide this complete tool to the MRI community.

We also thank all the members of the ICube imaging platform for their work and for the quality of their collaboration concerning the experimental part of this work. Experimental images were acquired at University of Strasbourg, CNRS, ICube, FMTS, Strasbourg, FRANCE.

This research was funded by the french Agence Nationale de la Recherche (VIVABRAIN project, Grant Agreement ANR-12-MONU-0010).

7. References

[1] J. Bittoun, J. Taquin, M. Sauzade, A computer algorithm for the simulation of any nuclear magnetic resonance (NMR) imaging method, Magnetic resonance imaging 2 (2) (1984) 113–120.

[2] L. Hanson, A graphical simulator for teaching basic and advanced MR imaging techniques, Radiographics 27 (6) (2007) e27.

[3] I. Marshall, Computational simulations and experimental studies of 3D phase-contrast imaging of fluid flow in carotid bifurcation geometries, Journal of Magnetic Resonance Imaging 31 (4) (2010) 928–934.

[4] S. Lorthois, J. Stroud-Rossman, S. Berger, L.-D. Jou, D. Saloner, Numerical simulation of magnetic resonance angiographies of an anatomically realistic stenotic carotid bifurcation, Annals of Biomedical Engineering 33 (3) (2005) 270–283.

[5] K. Jurczuk, M. Kretowski, J.-J. Bellanger, P.-A. Eliat, H. Saint-Jalmes, J. Bezy-Wendling, Computational modeling of MR flow imaging by the lattice Boltzmann method and Bloch equation, Magnetic Resonance Imaging 31 (7) (2013) 1163–1173.

[6] H. Benoit-Cattin, G. Collewet, B. Belaroussi, H. Saint-Jalmes, C. Odet, The SIMRI project: A versatile and interactive MRI simulator, Journal of Magnetic Resonance 173 (1) (2005) 97–115.

[7] T. H. Jochimsen, A. Schafer, R. Bammer, M. E. Moseley, Efficient simulation of magnetic resonance imaging with Bloch-Torrey equations using intra-voxel magnetization gradients, Journal of Magnetic Resonance 180 (1) (2006) 29–38.

[8] I. Drobnjak, D. Gavaghan, E. Sli, J. Pitt-Francis, M. Jenkinson, Development of a functional magnetic resonance imaging simulator for modeling realistic rigid-body motion artifacts, Magnetic Resonance in Medicine 56 (2) (2006) 364–380.

[9] C. Xanthis, I. Venetis, A. Aletras, High performance MRI simulations of motion on multi-GPU systems, Journal of Cardiovascular Magnetic Resonance 16 (1) (2014) 48.

[10] T. Stocker, K. Vahedipour, D. Pflugfelder, N. J. Shah, High-performance computing MRI simulations, Magnetic Resonance in Medicine 64 (1) (2010) 186–193.

[11] L. D. Jou, D. Saloner, A numerical study of magnetic resonance images of pulsatile flow in a two dimensional carotid bifurcation: A numerical study of MR images, Medical Engineering & Physics 20 (9) (1998) 643–652.

[12] P. Shkarin, R. G. S. Spencer, Time domain simulation of Fourier imaging by summation of isochromats, Imaging Systems and Technology 8 (1997) 419–426.

[13] M. Tambasco, D. A. Steinman, On assessing the quality of particle tracking through computational fluid dynamic models, Journal of Biomechanical Engineering 124 (2) (2002) 166–175.

[14] I. Marshall, Pulse sequences for steady-state saturation of flowing spins, Journal of Magnetic Resonance 133 (1) (1998) 13–20.

[15] C. Xanthis, I. Venetis, A. Chalkias, A. Aletras, MRISIMUL: a GPU-based parallel approach to MRI simulations, IEEE Transactions on Medical Imaging 33 (3) (2014) 607 – 617.

[16] M. Stevanov, J. Baruthio, B. Eclancher, Fabrication of elastomer arterial models with specified compliance, Journal of applied physiology 88 (4) (2000) 1291–1294.

[17] E. P. Durand, O. Jolivet, E. Itti, J. P. Tasu, J. Bittoun, Precision of magnetic resonance velocity and acceleration measurements: theoretical issues and phantom experiments, Journal of Magnetic Resonance Imaging 13 (3) (2001) 445–451.

[18] M. A. Bernstein, Y. Ikezaki, Comparison of phase-difference and complex-difference processing in phase-contrast MR angiography, Journal of Magnetic Resonance Imaging 1 (6) (1991) 725–729.

[19] I. Marshall, Simulation of in-plane flow imaging, Concepts in Magnetic Resonance 11 (6) (1999) 379–392.

[20] S. Petersson, P. Dyverfeldt, R. Gardhagen, M. Karlsson, T. Ebbers, Simulation of phase contrast MRI of turbulent flow, Magnetic Resonance in Medicine 64 (4) (2010) 1039–1046.